Drivetrain Reliability Collaborative 1.5 (DRC1.5) Project: Joint Industry Megawatt Scale Gearbox Field Tests

Cooperative Research and Development Final Report

CRADA Number: CRD-17-00702

NREL Technical Contacts: Yi Guo and Jon Keller

NREL is a national laboratory of the U.S. Department of Energy
Office of Energy Efficiency & Renewable Energy
Operated by the Alliance for Sustainable Energy, LLC

This report is available at no cost from the National Renewable Energy Laboratory (NREL) at www.nrel.gov/publications.

Contract No. DE-AC36-08GO28308

Technical Report
NREL/TP-5000-81066
September 2021

Drivetrain Reliability Collaborative 1.5 (DRC1.5) Project: Joint Industry Megawatt Scale Gearbox Field Tests

Cooperative Research and Development Final Report

CRADA Number: CRD-17-00702

NREL Technical Contacts: Yi Guo and Jon Keller

Suggested Citation
Guo, Yi, and Jon Keller. 2021. *Drivetrain Reliability Collaborative 1.5 (DRC1.5) Project: Joint Industry Megawatt Scale Gearbox Field Tests: Cooperative Research and Development Final Report, CRADA Number CRD-17-00702.* Golden, CO: National Renewable Energy Laboratory. NREL/TP-5000-81066. https://www.nrel.gov/docs/fy21osti/81066.pdf.

NREL is a national laboratory of the U.S. Department of Energy
Office of Energy Efficiency & Renewable Energy
Operated by the Alliance for Sustainable Energy, LLC

This report is available at no cost from the National Renewable Energy Laboratory (NREL) at www.nrel.gov/publications.

Contract No. DE-AC36-08GO28308

Technical Report
NREL/TP-5000-81066
September 2021

National Renewable Energy Laboratory
15013 Denver West Parkway
Golden, CO 80401
303-275-3000 • www.nrel.gov

NOTICE

This work was authored by the National Renewable Energy Laboratory, operated by Alliance for Sustainable Energy, LLC, for the U.S. Department of Energy (DOE) under Contract No. DE-AC36-08GO28308. Funding provided by U.S. Department of Energy Office of Energy Efficiency and Renewable Energy Wind Energy Technologies Office. The views expressed herein do not necessarily represent the views of the DOE or the U.S. Government.

This report is available at no cost from the National Renewable Energy Laboratory (NREL) at www.nrel.gov/publications.

U.S. Department of Energy (DOE) reports produced after 1991 and a growing number of pre-1991 documents are available free via www.OSTI.gov.

Cover Photos by Dennis Schroeder: (clockwise, left to right) NREL 51934, NREL 45897, NREL 42160, NREL 45891, NREL 48097, NREL 46526.

NREL prints on paper that contains recycled content.

Cooperative Research and Development Final Report

Report Date: September 22, 2021

In accordance with requirements set forth in the terms of the CRADA agreement, this document is the final CRADA report, including a list of subject inventions, to be forwarded to the DOE Office of Scientific and Technical Information as part of the commitment to the public to demonstrate results of federally funded research.

Parties to the Agreement: SKF USA Inc.

CRADA Number: CRD-17-00702

CRADA Title: Drivetrain Reliability Collaborative 1.5 (DRC1.5) Project: Joint Industry Megawatt Scale Gearbox Field Tests

Responsible Technical Contact at Alliance/National Renewable Energy Laboratory (NREL):

Yi Guo | yi.guo@nrel.gov (lead author and PI)

Jonathan Keller | jonathan.keller@nrel.gov (co-author and original PI)

Name and Email Address of POC at Company:

Dayananda Raju | dayananda.raju@skf.com

DOE Program Office:

Office of Energy Efficiency and Renewable Energy (EERE), Wind Energy Technologies Office

Joint Work Statement Funding Table showing DOE commitment:

Estimated Costs	NREL Shared Resources a/k/a Government In-Kind
Year 1	$335,000.00
Year 2	$300,000.00
Year 3	$300,000.00
TOTALS	$935,000.00

Executive Summary of CRADA Work:

A new Department of Energy (DOE)/NREL industry collaboration called the Drivetrain Reliability Collaborative 1.5 (DRC1.5) will undertake field testing on a commercial multi-megawatt wind turbine drivetrain to collect loading data as installed in the turbine to thoroughly characterize drivetrain loads and responses during actual in-field conditions. A chief outcome is to provide publicly available operational loading data to the industry. This will provide a greater understanding of steady-state, transient, and fault response for both the input and output of the drivetrain; thus, facilitating improvements in the drivetrain components, lubrication system, power converter or turbine controller.

Summary of Research Results:

The NREL Drivetrain Reliability Collaborative (DRC) was initiated by the DOE and developed with broad participation from the wind turbine industry to address the fact that wind turbine drivetrains are not achieving the expected 20-year design life. The DRC approach is to document and review the complete design process–from design to operational measurements to design validation–and identify the areas critical to design success that have high sensitivities or uncertainties. To date, not enough load and motion data has been collected from installed, commercial turbines during actual in-field conditions to thoroughly characterize main bearing loads and responses. The primary objective of this CRADA project was to measure the operational conditions on the main bearing in an installed wind turbine drivetrain to characterize the bearing wear and micropitting.

The main bearing is a critical component for which replacement typically requires specialized, expensive heavy lifting capabilities. A common drivetrain configuration in many land-based wind plants is a “three-point” mount, in which a double-row spherical roller bearing (SRB) functions as the main bearing and primarily supports the rotor weight and forces and the two gearbox torque arms supports the torque and rotor moments. The three-point configuration is cost-effective, allows for misalignment, and is easy to maintain because it is modular. However, the failure rate for many of these SRBs has been higher than expected, often as high as 20% to 30% in as short as 6 to 10 years [1], when originally designed for a rating life in excess of 20 years. Main bearing abrasion and wear, not accounted for in the design life estimation process, is one important potential root cause of failures.

One of the popular hypotheses for the cause of this wear is that axial movement between the roller and raceway breaks down the lubricant film thickness in the contact. Thus, it is essential to measure and understand this axial motion during turbine operations for improving main bearing and gearbox service life and reducing drivetrain O&M costs. The goals of this CRADA are to understand the operating conditions for the main SRB in a three-point drivetrain, including loads, and axial displacements and velocities; compare the measured values against a damage threshold defined by the CRADA partner SKF based on their numerical investigations; and use the analysis results to validate or disapprove this hypothesis for main bearing wear.

SKF USA Inc. (SKF) and NREL collaborated under this CRADA from January 2018 to March 2021. During this period, Jonathan Keller was the original NREL Principal Investigator (PI) for the project and Dayananda Raju was the SKF PI. Yi Guo assumed NREL PI duties in January 2020. As a part of this effort, a specially instrumented SKF main bearing was installed in the DOE-owned General Electric 1.5 megawatt (MW) SLE wind turbine at the Flatirons Campus in December 2017. After commissioning, the system was used to collect gearbox and bearing data from January 2018 until the conclusion of this CRADA. At the conclusion of this CRADA, the SKF main bearing remains installed in the turbine.

Through the course of the project, multiple tasks were completed and are summarized in this final report for the CRADA. Task descriptions in this report follow the numbering in the Joint Work Statement of the CRADA.

Task 1a Engineering Support for Instrumentation Development

Includes the following three subtasks:

1. *Participate in the collaborative to identify test goals and approach*
2. *Provide input and guidance to the collaborative on bearing design and manufacturing issues*
3. *Provide detailed bearing information for instrumentation purposes – specification, loads, ratings, drawings, models.*

This task was divided into two parts. Early on in the project, SKF provided NREL engineering support in the form of detailed information, including specifications, loads, ratings, drawings, and models, on the selected SKF main bearing for the purpose of developing the instrumentation for the bearing.

Task 2 Bearing Hardware and Instrumentation

Includes the following three subtasks:

1. *Provide test bearings for use in operation*
2. *Provide instrumentation for measurements of specific interest to the bearing supplier (i.e. roller slip, stray current, humidity and water-in-oil)*
3. *Provide in situ calibration assistance, if necessary.*

In this task, SKF provided the specially instrumented main bearing. It is a new spherical roller bearing (SRB) Wind bearing model BS2-8115/C2H. Although similar to a standard 240/600 ECA/W33 double-row series SKF Explorer SRB, its design was updated to optimize internal geometry specific to the turbine loads, use a new cage design and material, provide better sealing through a customized seal design, and improve lubrication with an automated relubrication system [2]. It is housed in a SKF model HC-Z 7051 BF housing. The main bearing and associated instrumentation are shown in Figure 1. Four inductive proximity sensors, equally spaced around the circumference of a custom frame installed on the generator-side of the main bearing housing, measure the axial displacement of the main bearing locknut (and bearing inner ring) with respect to the main bearing housing (and bearing outer ring). When the main shaft and bearing inner ring move downwind, the distance between the locknut and the sensors and frame mounted on the bearing housing decreases. The proximity sensors were installed at the midpoint

of their 10-mm measurement range relative to the locknut, and they have a repeat accuracy of ±0.02 mm. This measurement method has the advantage that it is not affected by elastic deformation of the bearing housing or bedplate. Combined with measurement of the main shaft azimuth, the axial displacement can be resolved to account for out-of-flatness of the custom frame, locknut and pivoting of the main shaft, which is essential to precisely determine main shaft axial displacement [3,4]. Rogowski coils attached to both sides of the main bearing housing measure any stray electrical current being conducted through the main shaft and main bearing. Separately, a total of eight design verification support tool (DVST) sensors, split evenly between the two sides of the main bearing, measure strain, acoustic emission, vibration, and temperature at four locations around the circumference of each bearing row. Finally, a standard SKF IMx-8 condition monitoring system was installed on the drivetrain, measuring vibration at two locations on the main bearing, five on the gearbox, and one on the generator [5].

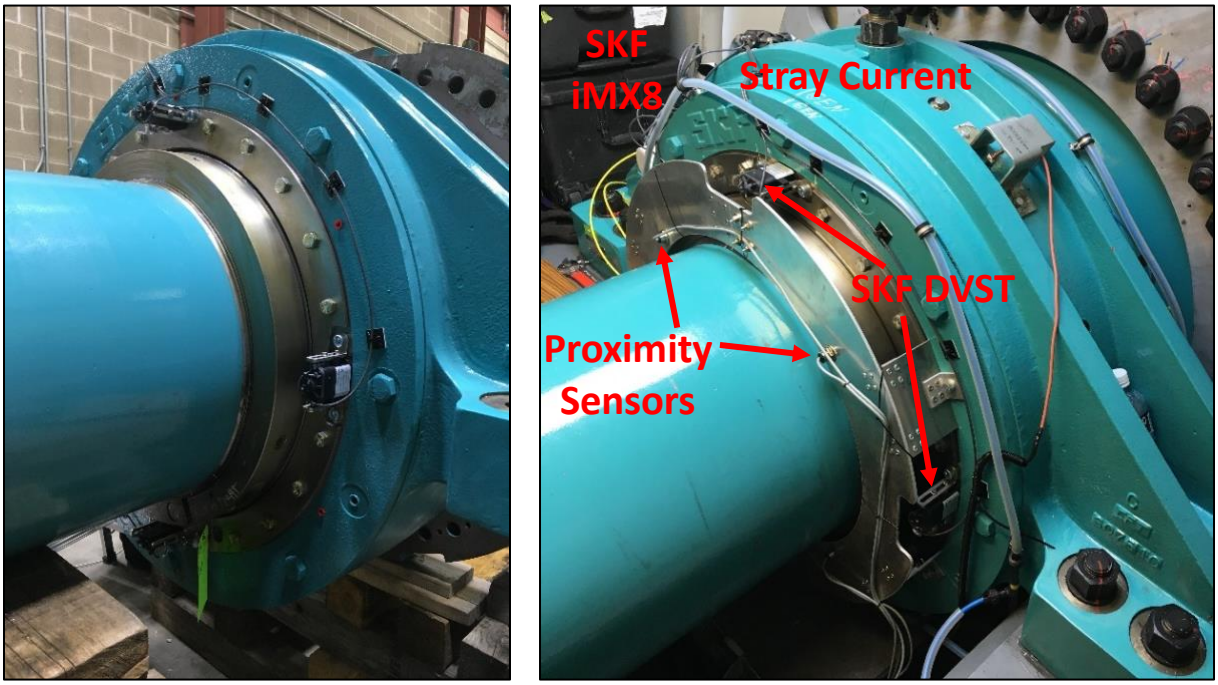

Figure 1. SKF SRB-Wind main bearing (left) and instrumentation (right). Photos by Jonathan Keller and Jerry Hur, NREL 49379 and 49959

The drivetrain was then installed in the GE 1.5-MW SLE wind turbine at the NREL Flatirons campus, as shown in Figure 2, in December of 2017. Gearbox measurements are time-synchronized with measurements from previously existing instrumentation on a meteorological tower in front of the turbine and on the turbine itself, including air temperature, pressure, and humidity; wind speed and direction at several heights, plus nacelle direction, rotor speed, and blade pitch angles; main shaft, tower, and blade loads; turbine power; and several supervisory control and data acquisition (SCADA) channels. The turbine and other instrumentation were recommissioned in January 2018, with full operations beginning in February 2018 [5,6].

Figure 2. Gearbox swap (left) and installation in turbine (right). Photos by Dennis Schroeder, NREL 49409 and 49413

Since then, drivetrain and turbine measurements have been acquired over a wide range of operating conditions, including power production in normally occurring winds; parked and idling situations; and intentionally induced transient startup, shutdown, emergency stop, and grid events. From installation through January 2021 (3 full years), the turbine was operated (i.e. connected to the grid and producing power) for over 4,200 hours.

Task 1b Engineering Support for Data Analysis

Includes the following subtask:

4. *Provide data analysis and interpretation supported by advanced bearing simulations*

Throughout the operation of the drivetrain and turbine, SKF and NREL collaborated on analysis of the data and interpretation of the results. Stray current measurements on either side of the main bearing were briefly characterized [5]. The majority of the analysis focused on developing a thorough understanding of the axial motion of the main bearing. Post-processing of the axial displacement measurements is required to yield the most accurate motion results [7]. With the displacements recorded by the four inductive sensors, the axial displacement of the inner ring with respect to the bearing housing (representative of the bearing outer ring) can be determined through the following steps:

- Remove the spurious readings caused by a gap in the locknut
- Estimate the readings in this region with a piecewise cubic Hermite interpolation
- Convert to units of mm
- Remove the influence of the misalignment and out-of-flatness of the retaining nut and locknut using measurements from slow rotations of the rotor
- Apply a 2.5-hertz (Hz) low-pass filter to reduce noise
- Average the four resulting signals, which remove any influence of pivoting of the shaft, to determine the main bearing axial displacement
- Subtract gravity-induced displacement from the axial displacement.

This data analysis was supported by development of a quasi-static bearing model that describes the main bearing displacement subject to gravity, inertial, and aerodynamic forces from the rotor. The model assumes that the system only translates in the axial direction, there is no damping, the reaction loads at the main bearing and bushings in the gearbox torque arms are represented as spring stiffnesses acting in a parallel arrangement, and there are no reaction loads from the generator coupling. A schematic of the drivetrain and relevant loads are shown in Figure 3. The degree of freedom of interest is the motion of the main bearing inner ring (and drivetrain) with respect to the fixed outer ring in the axial (x) direction [7].

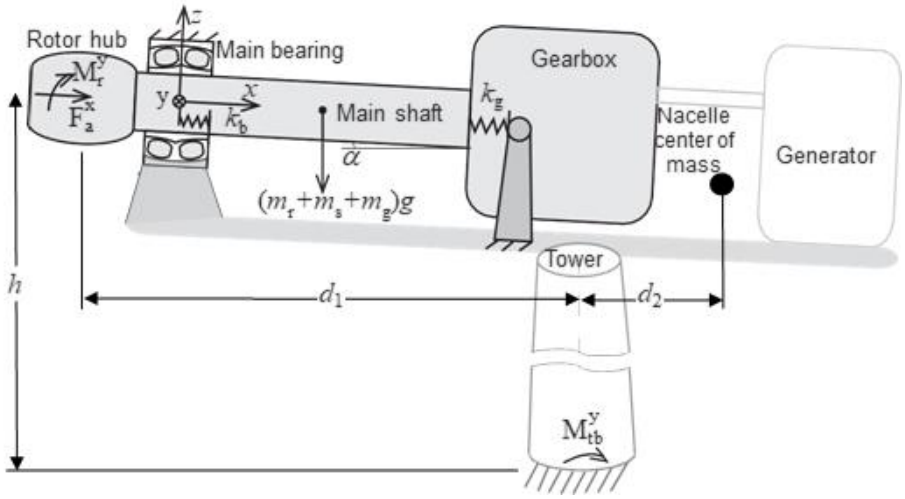

Figure 3. Force diagram of the wind turbine system

The axial load applied to the main bearing, F_a^x , and gravity loads resulting from the rotor, shaft, and gearbox masses, m_r, m_s and m_g, and the drivetrain tilt angle, □, are balanced by the spring stiffnesses of the main bearing, k_b, and the gearbox torque arms, k_g. Under gravity, the main bearing displaces downwind to a resting position. The main bearing motion described in this work is most easily interpreted with respect to this resting position, the condition for which is easily measured when the rotor is at a standstill or slowly idling. In comparison, the condition for which the main bearing is at its geometric center is not common and only occurs in negative thrust conditions. The axial motion of the bearing is then calculated from the applied axial load (typically the aerodynamic rotor thrust) as predicted from a simulation code, such as OpenFAST, or estimated from a force and moment balance using the measured blade and tower base moments, M_r^y and M_{tb}^y, on the turbine [7].

Nearly 400 data acquisitions limited to between 6 seconds (s) and 15 s, or approximately 2–5 shaft revolutions, in length were examined as shown in Figure 4. Data were acquired over almost the full power curve of the turbine, from very low wind speeds with light loads at cut in at 3.5 meters per second (m/s) wind speed to nearly the cut-out at 25 m/s. The aerodynamic rotor thrust reaches a maximum of approximately 225 kilonewton (kN) at 10 to 11 m/s wind speed and reduces as the wind speed increases beyond this point. The estimated aerodynamic rotor thrust is also compared to the prediction from the aero-servo-elastic simulation tool, OpenFAST, for steady wind in each case. There is good agreement between the predicted mean aerodynamic rotor thrust and the OpenFAST result. The measured axial displacement generally follows the same shape as the aerodynamic rotor thrust curve with the maximum axial displacement

occurring at approximately 10 m/s wind speed. Overall, the main bearing moves downwind up to 0.85 millimeter (mm) from its resting position under gravity. Above 10 m/s, the aerodynamic rotor thrust and the axial displacement decreases; however, the model predicts fairly constant displacements [7-9].

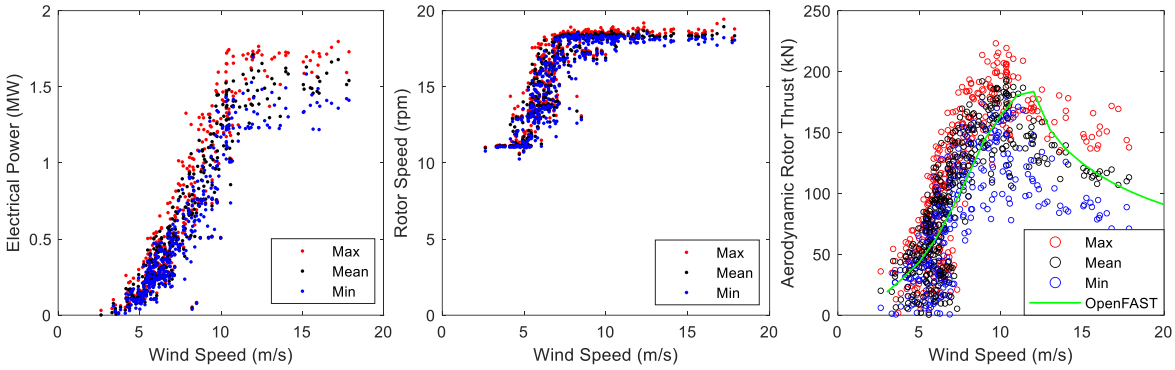

Figure 4. Measured electrical power (a), measured rotor speed (b), and predicted aerodynamic rotor thrust (c) during normal power production.

A statistical summary of the measured and predicted main bearing axial velocity is shown in Figure 5. The average velocity is less than 0.5 mm/s, but it can reach as much as 2 mm/s in some cases. Note that the turbulence intensity for this wind site varies tremendously—as high as 45% at low wind speeds and dropping to an average of approximately 15% at higher wind speeds. Ambient temperatures at the site also can range from approximately -20°C–35 °C, which can change the temperatures of and the resulting temperature gradients between the bearing rings, main shaft, and housing. As a result, the bearing operating axial clearance is expected to vary to some extent during long periods of normal power production and throughout the year. The analytic model estimations compare favorably to the experimental results, but—like the displacements—the velocities are lower than measured at higher wind speeds.

Finally, these relative velocities of the inner and outer rings can be compared to the roller rotational speed, assuming no slip. Generally, the relatively large radial load on the main bearing resulting from the rotor weight should be sufficient to ensure that this condition is met within the load zone. The speed of the roller surface, rotating about the center of the roller, ranges from 200–352 mm/s, which is generally two to three orders of magnitude larger than the relative axial velocity of the main bearing inner and outer rings. In addition to these steady-state conditions, a start-up, an idling, an emergency stop operation were also examined. Although these events are more dynamic in nature, the measured axial velocities were also less than 2 mm/s [7-9]. Previous simulations by SKF have shown that the axial speed between the ring and rollers is approximately 25% of the relative axial velocity between the bearing rings, equating to well less than 1 mm/s axial roller sliding. When compared to the speed of rolling, also shown in Figure 5, on the order of 200 to 352 mm/s the measured axial sliding is therefore less than 1% of the speed of rolling. The previous numerical studies of lubricant film formation in rolling contacts have shown that the effect of axial sliding only starts to be noticeable when this ratio exceeds 10%, so this is a small disturbance to the nominal pure rolling case and the influence on oil film building can be neglected.

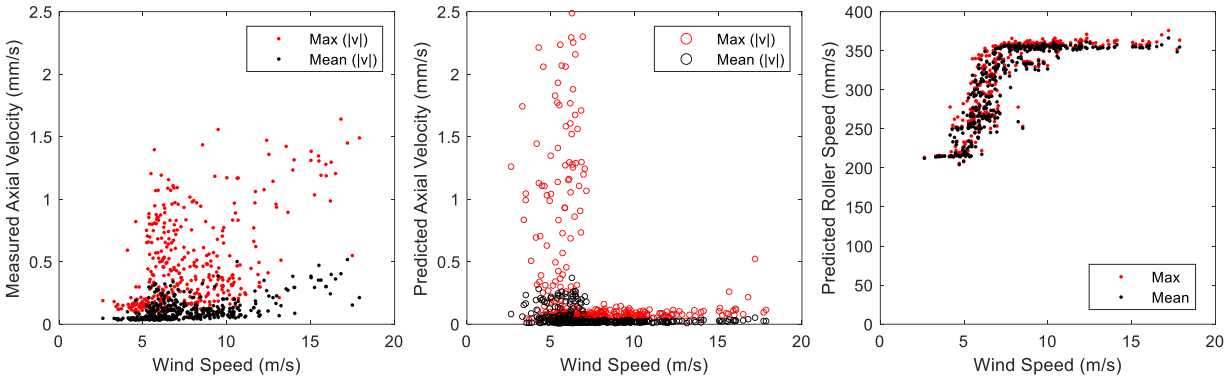

Figure 5. Measured axial velocity (left), predicted axial velocity (center), and predicted roller speed (right) during normal power production

Example time histories of stray electrical currents measured on both sides of the main bearing are shown in Figure 6. In general, these measurements exhibited noncontinuous, near-symmetric time-varying oscillations of current on the order of tens to hundreds of milliampere (mA).

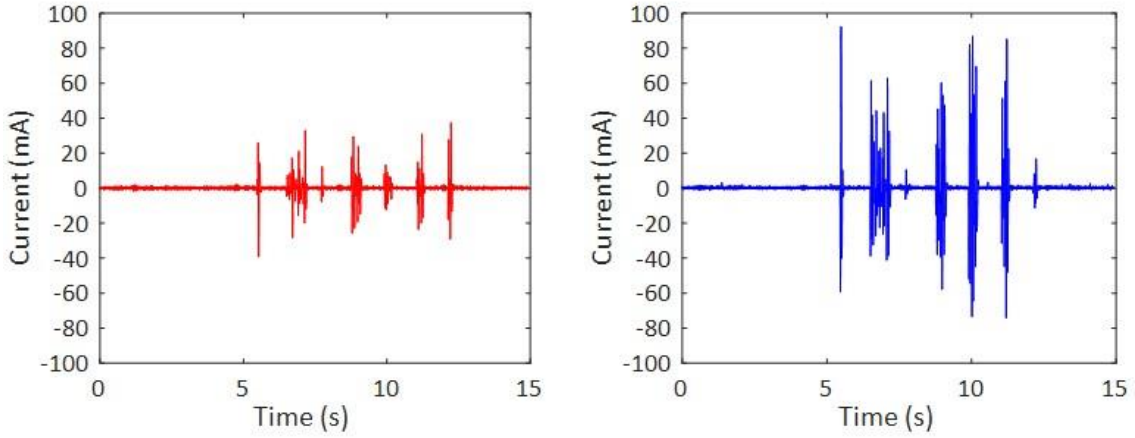

Figure 6. Main bearing generator-side (left) and rotor-side (right) electrical current in a normal power production case

The descriptive statistics for the maximum, minimum, and root-mean-square (RMS) level of main bearing electrical current on both sides of the main bearing across the range of normal power cases are shown in Figure 7. The correlation between these measurements and blade pitch motor activity [4] or other parameters is still being investigated; however, the largest currents up to almost 800 mA were observed on the rotor-side sensor in the variable speed operating region for the turbine from 3.5 to 14 m/s. The measurements on the generator-side sensor are similar, but lower in magnitude. The RMS current is on the order of 10 mA because of the noncontinuous nature of the measurement as seen in the previous figure.

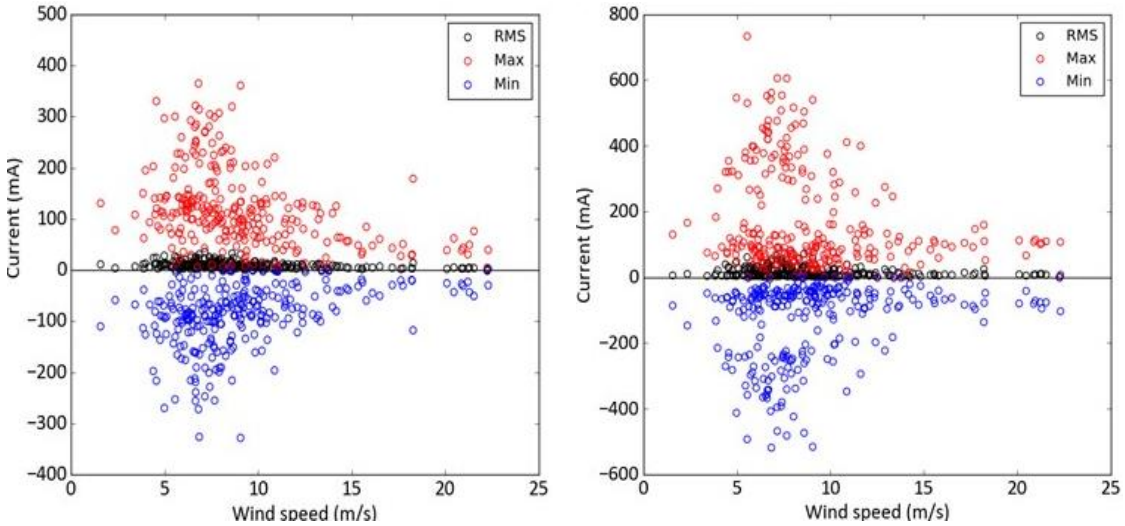

Figure 7. Main bearing generator-side (left) and rotor-side (right) stray electrical current in normal power production

Finally, over its first two years of operation, the main bearing was inspected twice and the grease sampled approximately every 6 months. Borescope images of the load zone taken during the second year of operation showed that the rollers (running surface and ends), cage, and inner and outer raceways were all in good condition as shown in Figure 8. The grease samples also noted no anomalies.

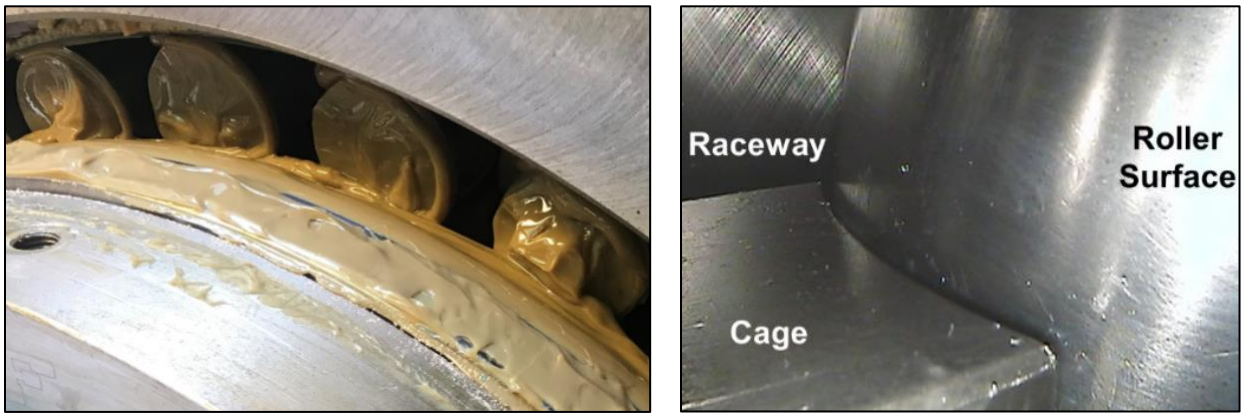

Figure 8. Inspection results of main bearing downwind row. Photos by Mark Dunn, SKF USA Inc., NREL 63050 and 63052

References:

1. Sethuraman, L., Y. Guo, and S. Shuangwen. 2015. Main Bearing Dynamics in Three-point Suspension Drivetrains for Wind Turbines (Presentation). NREL/PR-5000-64311. National Renewable Energy Laboratory (NREL), Golden, CO (US). https://www.nrel.gov/docs/fy15osti/64311.pdf.

2. James, P. 2018. Optimized Spherical Roller Bearing for Wind Turbine Rotors. Presented at the Drivetrain Reliability Collaborative Meeting. Feb 21. https://www.dropbox.com/s/1vu6t47fovgaysh/03%20Optimized%20Spherical%20Roller%20Bearing.pdf?dl=0.

3. Wendeberg, H. 2016. Axial Motion in Wind Turbine Main Shaft Spherical Roller Bearings. Presented at the Wind Turbine Tribology Seminar. Nov. 16.

4. Raju, D., and O. Bankestrom. 2017. A System Approach to address Main Bearing Reliability. Presented at the Drivetrain Reliability Collaborative Meeting. Feb 21. https://www.dropbox.com/s/q1j8aag6oyz6490/03%20A%20System%20Approach%20to%20Address%20Main%20Bearing%20Reliability.pdf?dl=0.

5. Keller, J., Y. Guo, and L. Sethuraman. 2019. Uptower Test Report for the Investigation of Main and High-Speed Shaft Bearing Reliability (Technical Report). NREL/TP-5000-71529. National Renewable Energy Laboratory (NREL), Golden, CO (US). http://www.nrel.gov/docs/fy19osti/71529.pdf.

6. Keller, J. 2018. Investigating Main and High-Speed Shaft Bearing Reliability Through Uptower Testing (Presentation). NREL/PR-5000-70958. National Renewable Energy Laboratory (NREL), Golden, CO (US). http://www.nrel.gov/docs/fy18osti/70958.pdf.

7. Bankestrom, O., Y. Guo, R. Bergua, J. Keller, and M. Dunn. 2021. "Investigation of Main Bearing Operating Conditions in a Three-Point Mount Wind Turbine Drivetrain." *Forschung im Ingenieurwesen (Springer)*, https://doi.org/10.1007/s10010-021-00477-8.

8. Bankestrom, O. 2021. Investigation of main bearing operating conditions in a three-point mount wind turbine drivetrain. Presented at the Drivetrain Reliability Collaborative Meeting. Feb 16.

9. Bankestrom, O., Y. Guo, R. Bergua, J. Keller, and M. Dunn. 2021. Investigation of Main Bearing Operating Conditions in a Three-Point Mount Wind Turbine Drivetrain (Presentation). NREL/PR-5000-79442. National Renewable Energy Laboratory (NREL), Golden, CO (US). http://www.nrel.gov/docs/fy21osti/79442.pdf.

Subject Inventions Listing:

None

ROI #:

None